

## EXPERIMENTAL INVESTIGATION OF AN ACETONE LOOP HEAT PIPE USING A CERAMIC POROUS WICK IN THE CAPILLARY EVAPORATOR

**Paulo Henrique Dias dos Santos**, paulosantos@labcet.ufsc.br

**Edson Bazzo**, ebazzo@emc.ufsc.br

Federal University of Santa Catarina, Department of Mechanical Engineering  
LabCET - Laboratory of Combustion and Thermal Systems Engineering  
Campus Universitário, 88.040-900, Florianópolis, SC, Brazil

**Rainer Mertz**

University of Stuttgart, Department of Mechanical Engineering  
IKE – Institute of Nuclear Technology and Energy Systems  
Pfaffenwaldring 31, 70569 Stuttgart, Germany  
rainer.mertz@ike.uni-stuttgart.de

**Abstract.** *The ceramic porous media is proposed as an alternative for LHP applications. Performance tests using acetone as the working fluid were carried out for power inputs up to 25 watts. The evaporator has a stainless steel cylindrical assembly, with 65 mm of length and 10 mm of diameter. The ceramic porous wick has 50% of porosity, 1 to 3  $\mu\text{m}$  of pore radius and permeability of about  $35\text{E-}15 \text{ m}^2$ . The active zone length of the evaporator is 25 mm. For a limited operation temperature of  $100^\circ\text{C}$ , the LHP was able to transfer up to 25W at steady state condition. An operation analysis concerning the effects of the LHP inclination and the heat sink temperature is also presented. Despite the good performance of the LHP, it was observed that further researches are still required taking into account changes related to properties of the ceramic porous wick and improvements in the whole LHP design.*

**Keywords:** *Ceramic porous wick, LHP, Acetone working fluid.*

### 1. INTRODUCTION

Thermal control has become a relevant issue of interest in modern computers due to their continuous size decreasing and power increasing requirements. The next generations of microprocessors will become more and more powerful and smaller and there will be a relative high need to find reliable and efficient devices for heat dissipation. Currently heat pipes or passive heat transfer devices have been also used for cooling purpose. However, heat pipes shall soon probably be improved or replaced by much higher heat transport capacity devices. The Loop Heat Pipes (LHP), which was previously developed for spacecraft thermal control system (Maydanik, 2005), are a reliable alternative and can also transport heat with high performance for terrestrial electronic cooling application.

LHPs are two-phase heat transfer devices, which work by capillary action to pump the working fluid. They have high heat transport capacity and work in a range of operation temperature, usually defined by the working fluid properties. Since the working fluid circulation is accomplished by the capillary action inside the evaporator, the pumping mechanism does not consume electric power. Besides this advantage, they have low thermal resistance to heat transfer and they do not have mechanical parts.

Many researchers have reported experimental studies related to the LHP operation conditions, such as Ku (1999), Chuang (2003), Pastukhov et al. (2003), Ku et al (2004), Chen et al. (2006), Pastukhov and Maydanik (2007) and Maydanik and Vershinin (2009). They have analyzed the thermal behavior and startup of LHPs in regard to the working fluid inventory, slopes of the LHP, wick material (nickel, stainless steel, copper, polyethylene), body material of the evaporator (copper and stainless steel), cooling system of condenser (forced convection using water and air, and natural convection using air), multi-evaporators and condensers, heat sink and environment temperatures at ground and microgravity conditions for a range of power inputs.

Nowadays there is no any LHP using ceramic porous wick as the evaporator capillary structure. Most LHPs use polyethylene or metallic porous wicks. However, it is supposed that ceramic wicks become more advantageous, because they are less expensive, easier to machine without damaging the pores in the

external surface of the structure. Also the low thermal conductivity can minimize the high radial heat leak to the liquid feeding channel mainly at high heat loads.

This paper presents a comprehensive experimental study of the thermal behaviour and startup of the LHP. The ceramic porous media is proposed as an alternative for this application. Performance tests using acetone as the working fluid were carried out for power inputs up to 25 watts. The evaporator has a stainless steel cylindrical assembly, with 65mm of length and 10 mm of diameter. The ceramic porous wick has 50% of porosity, 1 to 3  $\mu\text{m}$  of pore radius and permeability of about  $35\text{E-}15 \text{ m}^2$ . The active zone length of the evaporator is 25mm. For a limited temperature of  $100^\circ\text{C}$ , the LHP was able to transfer up to 25W at steady state condition. An operation analysis concerning the effects of the LHP inclination and the heat sink temperature is also presented.

## 2. LHP DESCRIPTION

A typical LHP is shown in Fig. 1, consisting of a capillary evaporator, a compensation chamber, a condenser and transport lines of liquid and vapor. Heat is supplied to the evaporator so that the liquid saturated into the wick evaporates, forming at the same time the menisci in the interface liquid-vapor that promote the fluid circulation as a result of the capillary forces, developed by the fluid surface tension. The vapor generated in the evaporator goes via vapor transport line to the condenser, where heat is removed and the vapor condenses. The fluid returns to the evaporator by the capillary forces action.

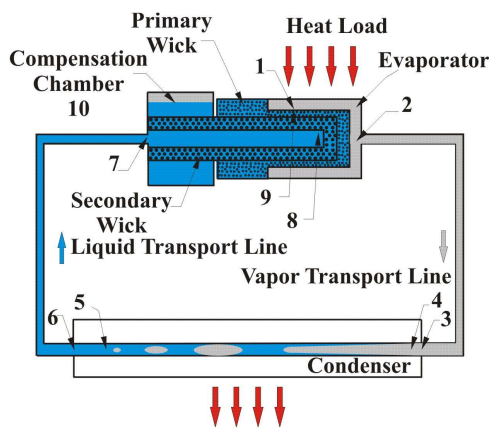


Figure 1. Functional schematic of a LHP.

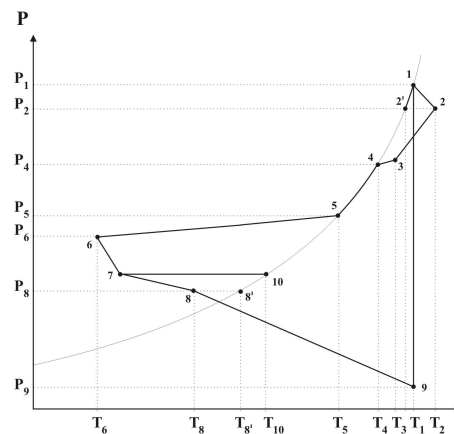


Figure 2. PT diagram for a LHP.

A PT diagram is depicted in Fig. 2 related to the LHP shown in Fig. 1. In the point 1, the liquid vaporizes at a saturation temperature  $T_1$ , corresponding to a pressure  $P_1$ . The generated vapor flows via the evaporator grooves causing a pressure drop due to the viscous friction from  $P_1$  to  $P_2$  in a close location of the evaporator outlet, where liquid vaporizes at a lower saturation temperature  $T_2'$ . Therefore, the liquid vaporizes along the external wick surface at a temperature small range between  $T_1$  and  $T_2'$ , instead of a fixed temperature  $T_1$ . The vapor leaves the evaporator at the superheated state (point 2), in part due to the decrease in the saturation pressure and in part due to the proximity of the hot source that supplies the system. The vapor continues to drop pressure as flows via vapor transport line. Between the points 2 and 3, the vapor experienced an expansion process and its temperature decreases lightly. The thermodynamic state of the entering vapor in the condenser is represented by the temperature  $T_3$  and pressure  $P_3$ . A small area of the condenser is enough to dissipate the sensible heat before the beginning of the vapor condensation in the point 4 at a pressure  $P_4$  (smaller than  $P_3$ ) and at a saturation temperature  $T_4$ .

The condensation happens between the points 4 and 5. In the point 5 there is no more vapor. Similar to the liquid vaporization into the evaporator, the vapor condensation occurs at a temperature range between  $T_4$  e  $T_5$ . The liquid continues to lose sensible heat up to reach a subcooled temperature  $T_6$  in the condenser outlet. The liquid temperature increases lightly, while the pressure decreases from  $P_6$  to  $P_7$  in the inlet of the liquid feeding channel into the evaporator. The PT diagram, shown in Fig. 2, presents an analysis for steady

state. Therefore there is no mass flow between the compensation chamber and the liquid feeding channel into the evaporator. Consequently, the saturation pressure  $P_{10}$  in the compensation chamber should be the same pressure  $P_7$ . Inside the liquid feeding channel, the temperature increases up to  $T_8$  as a consequence of the heat leak from the wick to the liquid. The point 8' represents the saturation state corresponding to the pressure  $P_8$ . The liquid in the external wick surface is heated and reaches the saturation temperature  $T_1$  corresponding to the pressure  $P_1$  before vaporizing. It is noticed by Fig. 2 that the liquid side of the menisci (point 9) is in its superheated state. The total pressure drop in the system is equal to the difference between  $P_1$  and  $P_9$ , which in its turn cannot be larger than the maximum capillary pressure head.

The maximum capillary pressure head ( $\Delta P_{cap,max}$ , Pa) is function of the fluid surface tension ( $\sigma$ , N/m), the effective porous radius of the wick ( $r_p$ , m) and the contact angle between the liquid and the wick ( $\theta = 0^\circ$ ):

$\Delta P_{cap,max} = \frac{2\sigma \cos \theta}{r_p}$	(1)
--	-----

The LHP operation requires that the sum of the pressure drops in the all components, including the transport lines and any static pressure drop due to gravity, must be smaller than the maximum capillary pressure head developed by the wick:

$\Delta P_{cap,max} \geq \Delta P_{evap} + \Delta P_{cond} + \Delta P_v + \Delta P_l + \Delta P_g$	(2)
--	-----

According to Ku (1999), in the most of the two-phase capillary pumping systems the changes of pressure and temperature are extremely small; therefore it can approach the saturation curve (PT diagram, Fig. 2) for a straight line between two points using the Clausius-Clapeyron equation:

$\left. \frac{dP}{dT} \right _{T_{sat}} = \frac{h_{lv}}{T_{sat} v_{lv}}$	(3)
--	-----

where:  $\left. \frac{dP}{dT} \right|_{T_{sat}}$  is the slope of the pressure-temperature saturation line [Pa/K],  $h_{lv}$  is the latent heat of vaporization [kJ/kgK],  $T_{sat}$  is the saturation temperature [K] e  $v_{lv}$  is the difference in specific volumes during vaporization [ $m^3/kg$ ].

According to Maydanik et al. (1991), taking for instance the points 1 (evaporator) and 10 (compensation chamber), the saturation line slope times the temperature differential between these two points of the curve is approximately equal to the pressure differential between them:

$\left. \frac{dP}{dT} \right _{T_{10}} (T_1 - T_{10}) \approx (P_1 - P_{10})$	(4)
---	-----

In any circumstance, the liquid vaporization temperature  $T_1$  is related to the saturation temperature of the compensation chamber  $T_{10}$  by the union of Eqs. (3 and 4):

$$(T_1 - T_{10}) = \frac{(P_1 - P_{10}) T_{10} v_{lv}}{h_{lv}} \quad (7)$$

According to the Eq. (7), it is expected that the LHP inclination influences its temperature operation. Any change in the pressure difference between the points 1 and 10 due to the LHP inclination will result in a saturation temperature difference changing between the evaporator and compensation chamber. Since  $T_{10}$  in

the compensation chamber does not change, the unique manner to satisfy the Eq. (7) is to increase the temperature  $T_1$ .

According to Santos and Bazzo (2007), the capillary pumping systems in the variable conductance mode can also work in fixed conductance mode. When these systems are operating at low thermal load condition, the compensation chamber is operating in the two-phase condition (variable conductance mode). When the thermal load increases, the condensation front moves forward, causing the liquid displacement from the condenser to the compensation chamber until this compartment is completely filled (fixed conductance mode). Figure (3) shows qualitatively how is the evaporator temperature profile for a LHP working in fixed and variable conductance modes as a function of the thermal load. Even in the variable conductance mode, the evaporator temperature does not remain constant and as the thermal load increases, the evaporator temperature decreases. This phenomenon occurs when the heat sink temperature is lower than the environment temperature. According to Chernysheva et al. (2007) two factors are responsible for this phenomenon: (i) decreasing of the condensation area, caused by the liquid displacement from the condenser to the compensation chamber; (ii) changing in the saturation temperature into the compensation chamber  $T_{10}$ , that influences directly in the change of the evaporation temperature, due to a complex process of heat and mass transfer.

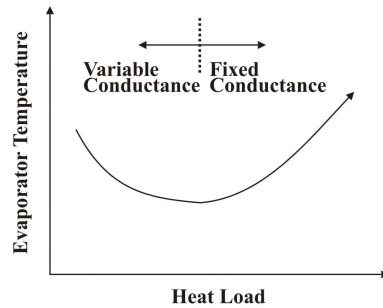


Figure 3. Typical curves of evaporator temperature for LHP in the fixed and variable conductance.

### 3. DESCRIPTION OF THE EXPERIMENTAL DEVICE

Figures (4a and b) show the proposed LHP which has a cylindrical capillary evaporator with 10mm of intern diameter and 28mm of length; a ceramic porous wick with 50% of porosity, 1 to 3  $\mu\text{m}$  and permeability of about  $35\text{E-}15 \text{ m}^2$ ; a compensation chamber with the same diameter of the evaporator and length of 32mm; transport lines of liquid and vapor with 2.8mm of intern diameter and a condenser with 100mm of length.

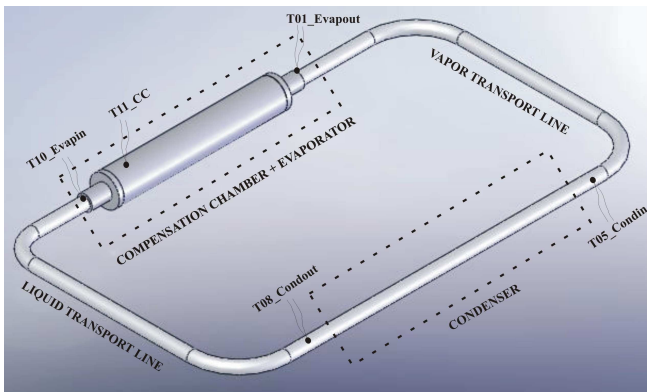


Figure 4a. Sketch of LHP and the positions of thermal resistors.

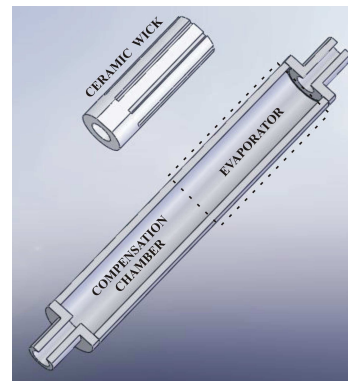


Figure 4b. Detailed sketch of the compensation chamber, capillary evaporator and ceramic porous wick assembly.

Figure (4a) presents the thermal resistors localizations on the evaporator and condenser inlets, condenser outlet, inlet of the assembly (compensation chamber and evaporator) and compensation chamber. Only the upper side of the capillary evaporator has grooves with rectangular format, as shown in Fig. (4b).

Figure (5a) depicts the LHP and the condenser box. The condenser was cooled using water in forced convection. The capillary evaporator was heated using a skin heater. Figure (5b) shows the compensation chamber, the evaporator and the details of wick grooves. The LHP was tested using an insulated box in which the environment temperature was controlled.

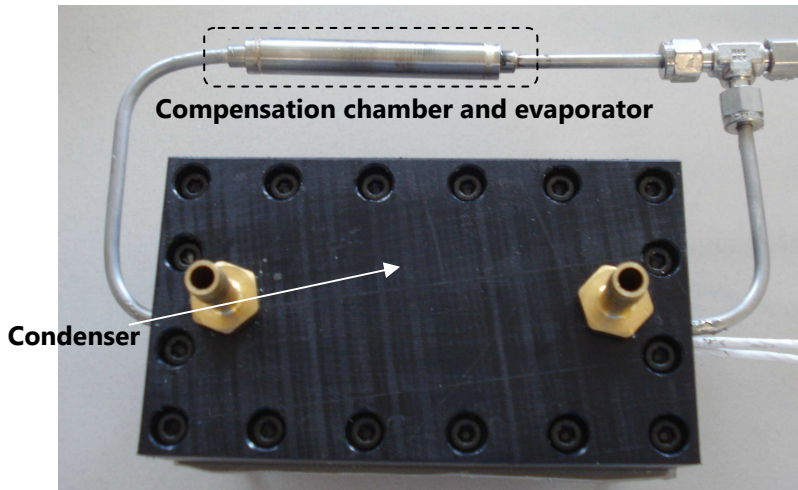


Figure 5a. View of LHP and the condenser box.

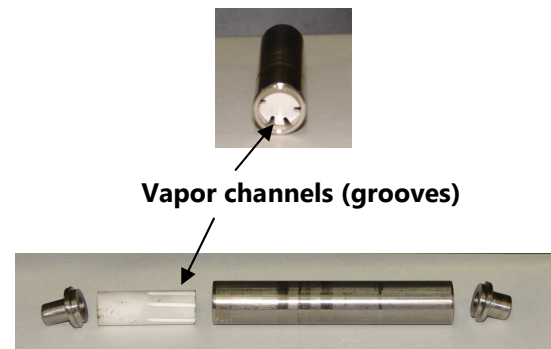


Figure 5b. View of the evaporator, the compensation chamber and the ceramic porous wick.

## 4. EXPERIMENTAL RESULTS

The performance tests were carried out for power inputs in the range of 5 to 25 watts, taking into account the influence of the working fluid inventory, changes in the heat sink temperature and also different slopes in relation to the horizontal position of the LHP. The environment temperature was controlled at  $20 \pm 0.5^\circ\text{C}$ . For safety reasons, the maximum operation temperature was limited to  $100^\circ\text{C}$ , resulting in a maximum power input of 25 W. As previously mentioned, acetone was used as the working fluid.

### 4.1 The working fluid inventory and startup

A successful startup has been related mainly to the applied heat load and heat sink temperature of the LHP. It is worthwhile to point out also the influence of the working fluid inventory. Figure (6) shows the start up for 50, 60, 65 and 70% working fluid charge ratio, under heat load of 10W and condenser positioned  $90^\circ$  above the evaporator. The startup was not successful for working fluid charge ratio less than 60%. As shown in Fig. (6a), for 10 W supplied power input, after approximately 60 s, the inlet condenser temperature increases fast, showing the vapor front reaching the condenser. At 130 s, however, the temperature starts to decrease, showing that the system failed. As a consequence, the outlet evaporator temperature increases continuously. A similar thermal behavior is shown in Fig. (6b), nevertheless the system failed at approximately 275 s. A successful startup was reached in case of 65% working fluid charge ratio (Fig. 6c). Both the outlet evaporator and the inlet condenser temperatures reached a steady state condition at 68 and  $56^\circ\text{C}$ , respectively. A better thermal behavior was achieved for 70% working fluid charge ratio, still for condenser positioned at  $90^\circ$  above the evaporator. Now the outlet evaporator and the inlet condenser temperatures reached the steady state condition at 52 and  $47^\circ\text{C}$ , respectively. It is evident the difference of operation temperatures between the cases (c) and (d). So, the fluid inventory plays an important role regarding the operating temperature of the LHP

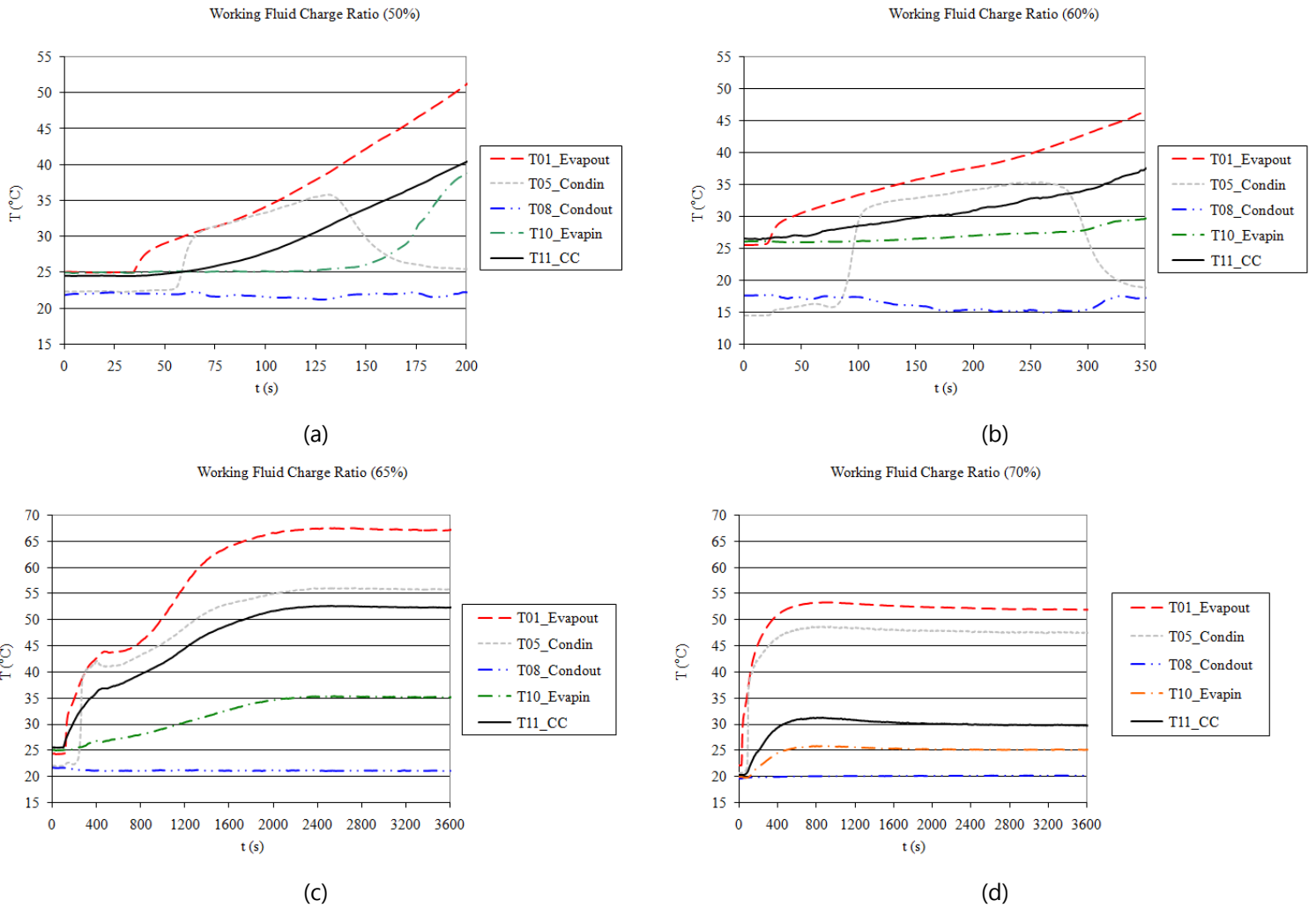


Figure 6 Startup under heat load of 10W and condenser positioned  $90^{\circ}$  above the evaporator, for working fluid charge ratio of 50% (a), 60% (b), 65% (c) and 70% (d)

The startup was fully successful also for LHP positioned in the horizontal position (Fig. 7). Again for 10 W power input and 70% working fluid charge ratio, now the outlet evaporator and the inlet condenser temperatures reached the steady state condition at 56 and  $54^{\circ}\text{C}$ , respectively. Again, the measured temperatures are not the same. As suggested by Eq. (7), the higher the total pressure drop of the loop the higher the evaporator temperature. So, without gravity assistance, the evaporator temperature increased from 52 to  $56^{\circ}\text{C}$ .

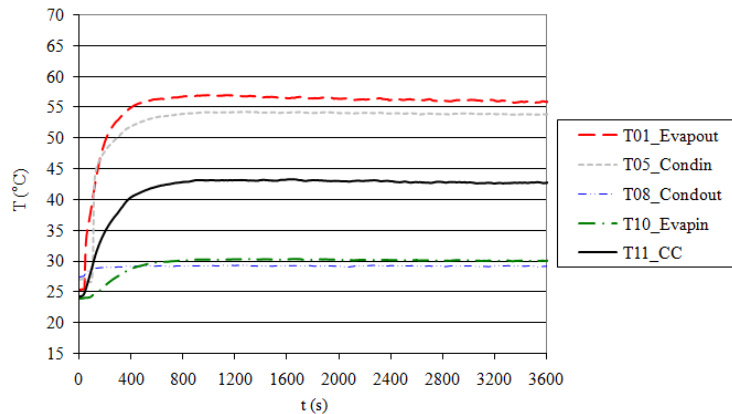


Figure 7. Startup for heat load of 10 W, LHP positioned in the horizontal position and working fluid charge ratio of 70%.

### 4.2 Steady state operation

The LHP has worked satisfactory in the range of 5 to 25 W. Figure (8) depicts the temperatures concerning the outlet evaporator, T01, inlet condenser, T05, outlet condenser, T08, inlet evaporator, T10, and the compensation chamber, T11.

The temperature limit of 100°C, as previously assumed for safety reasons, was reached for 25 W power input. The wall temperature along the vapor transport line changes as consequence of axial heat transfer from evaporator to the condenser section. Contrarily to capillary pumped loops, the temperature of the compensation chamber is not constant, changing from 29 to 51°C. The outlet evaporator temperature has been measured much higher, from 50 to 98°C, and the temperature difference related to the heat sink temperature (20°C), from 30 to 78°C. This condition is determinant for a successful application of this specific LHP. Therefore, high temperature differences claim for changes in the properties of the ceramic porous wick (porosity, pore size and thermal conductivity) or improvements in the original LHP design. The thermal resistance at the interface between the porous wick and inner diameter of the evaporator should also be considered.

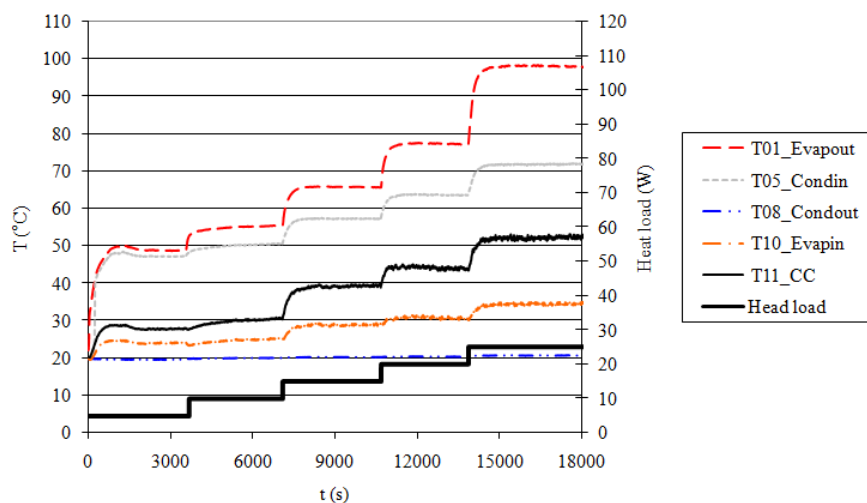


Figure 8. Steady state operation for heat load increasing at horizontal position and at heat sink temperature of 20°C.

As shown in Fig. (8), subcooled liquid enters in the evaporator at any power input. The evaporator temperature always increases indicating a fixed conductance behavior of the LHP at the tested conditions (see Fig. 3). However experimental results for heat sink temperatures below -10°C showed a variable conductance behavior (see Fig. 9), as already discussed before.

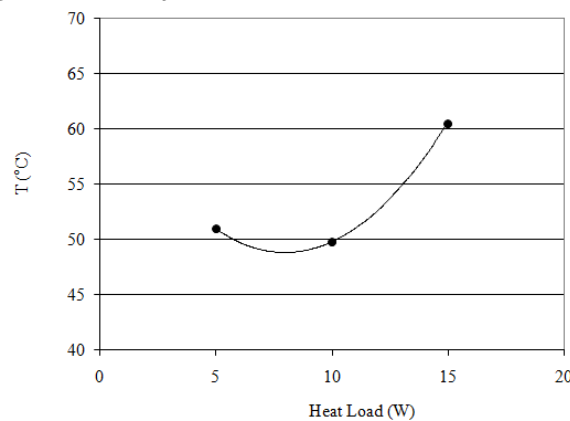


Figure 9. Outlet evaporator temperature for different power inputs and heat sink temperature of -10°C.

As also discussed before, the inclination has a relative influence on the thermal behavior of the LHP. Four different scenarios were analyzed: (i) condenser positioned 90° above the evaporator; (ii) condenser positioned 10° above the evaporator; (iii) evaporator positioned 10° above the condenser; (iv) evaporator positioned 90° above the condenser. In Fig. (10) is depicted the outlet evaporator temperature for heat loads ranging from 5 to 25 W. As expected, the lowest outlet evaporator temperature was measured for condenser positioned 90° above the evaporator. On the other side, the highest temperature was measured for evaporator positioned 90° above the condenser.

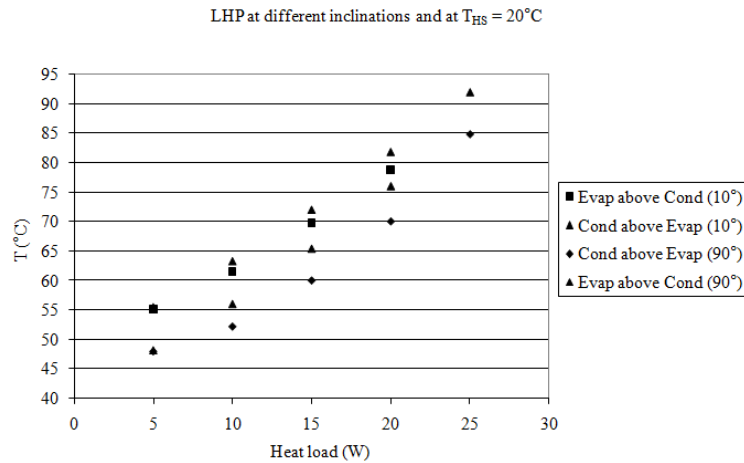


Figure 10. Influence of the inclination of the LHP.

## 5. CONCLUSION

The ceramic porous media is a reliable alternative for LHP applications. Performance tests with acetone were carried out for power inputs up to 25 watts, taking into account the influence of the working fluid inventory, changes in the heat sink temperature and also different slopes in relation to the horizontal position of the LHP. For higher power inputs, temperatures above 100°C were measured.

Further researches are still required in order to reduce the operation temperature, evaluating changes related to properties of the ceramic porous wick (porosity, pore size and thermal conductivity) and improvements in the whole LHP design.

## 6. ACKNOWLEDGMENTS

The authors thank the National Council for Scientific and Technological Development (CNPq), a foundation linked to the Ministry of Science and Technology (MCT), as well as to the German Academic Exchange Service (DAAD) by the financial support to carry out the experiments at the Institute of Nuclear Technology and Energy Systems (IKE) of University of Stuttgart.

## 7. REFERENCES

- Chen, Y., Groll, M., Mertz, R., Maydanik, Y. F. and Vershinin, S.V., 2006, "Steady-state and transient performance of a miniature loop heat pipe", *International Journal of Thermal Sciences*, Vol.45, pp. 1084-1090.
- Chernysheva, M. A., Vershinin, S. V. and Maidanik, Y. F., 2007, "Operating Temperature and Distribution of a Working Fluid in LHP", *International Journal of Heat and Mass Transfer*, Vol.50, pp. 2704-2713.
- Chuang, P. -Y. A., 2003, "An Improved Steady-State Model of Loop Heat Pipe Based on Experimental and Theoretical Analyses", PhD Thesis, Pennsylvania State University.
- Ku, J., 1994, "Thermodynamic Aspects of Capillary Pumped Loop Operation", *Proceedings of the 6th AIAA/ASME Joint Thermophysics and Heat Transfer Conference*, AIAA-94-2059, Colorado Springs, USA, pp.1-11.

Ku, J., 1999, "Operating Characteristics of Loop Heat Pipes", Proceedings of the 29th International Conference on Environmental System, 1999-01-2007, Denver, Colorado, USA.

Ku, J. Ottenstein, L. and Birur, G., 2004, "Thermal Performance of a Multi-Evaporator Loop Heat Pipe with Thermal Masses and Thermal Electrical Coolers", Proceedings of the 13th International Heat Pipe Conference (IHPC), Shanghai, China.

Maydanik, Y. F., Fershtater, Y. G. and Goncharov, K. A., 1991, "Capillary-pump Loop for the Systems of Thermal Regulation of Spacecraft", Proceedings of the 4th European Symposium on Space Environmental and Control Systems, Florence, Italy, pp. 87-92.

Maydanik, Y. F., 2005, "Loop Heat Pipe - Review", Applied Thermal Engineering, Vol. 25, pp. 635-657.

Maydanik, Y. F. and Vershinin, S.V., 2009, "Development and tests of ammonia Miniature Loop Heat Pipes with cylindrical evaporators", Applied Thermal Engineering, Vol. 29, pp. 2297-2301.

Pastukhov, V.G., Maydanik, Y. F., Vershinin, S.V. and Korukov, M.A., 2003, "Miniature loop heat pipes for electronics cooling", Applied Thermal Engineering, Vol. 23, pp. 1125-1135.

Pastukhov, V.G and Maydanik, 2007, "Low-noise cooling system for PC on the base of loop heat pipes", Applied Thermal Engineering, Vol. 27, pp. 894-901.

Santos, P. H. D. and Bazzo, E., 2007, "Thermohydraulic Analysis of Two-Phase Capillary Pumping Systems for Industrial Design and Space Applications", Proceedings of the 19th International Congress of Mechanical Engineering (COBEM), Brasília, Brazil.